Ali Vatanshenas
Structure and Environment 2025, vol. 17, (1), pp. 18-27, Article number: el 003
https://doi.org/10.30540/sae-2025-003

Structure and Environment
ISSN 2081-1500
e-ISSN 2657-6902
https://content.sciendo.com/sae
https://sae.tu.kielce.pl

sciendo

Kielce University of Technology

DOI: 10.30540/sae-2025-003

INVESTIGATING EFFECTIVENESS OF TUNED MASS DAMPER (TMD) ON CONTROL VIBRATION OF WIND TURBINE-SOIL INTERACTION

BADANIE EFEKTYWNOŚCI DYNAMICZNEGO TŁUMIKA DRGAŃ (TMD) POD KĄTEM KONTROLI WIBRACJI W INTERAKCJI TURBINY WIATROWEJ Z PODŁOŻEM GRUNTOWYM

Ali Vatanshenas*
Tampere University, Finland

Abstract

Soil-structure interaction (SSI) effects were investigated on structural responses of wind turbine. Force versus deformation (i.e., p-y curves) was simulated by multilinear elastic springs. The whole system, including the structure, control vibration system and soil nonlinear effects are simulated within a single three-dimensional finite element model. Modeling accuracy was verified using available results related to a 65 kW wind turbine discussed in the literature. Pushover analysis results indicated a fixed-base assumption ends up with overestimation of stiffness compared to the case where SSI effects are considered. Moreover, it is observed that the performance of tuned mass damper (TMD) is highly dependent on its tuned frequency domain, and its efficiency decreases significantly after SSI effects are considered. Lateral deformations of a wind turbine are much higher compared to the fixed-base condition. Therefore, SSI effects play a crucial part in designing wind turbines and should not be neglected in practice.

Keywords: dynamic analysis, pushover analysis, p-y curves, soil-structure interaction, tuned mass damper, wind turbine

Streszczenie

Zbadano wpływ interakcji konstrukcji z podłożem gruntowym (SSI) na zachowanie konstrukcji turbiny wiatrowej. Zależność siły od odkształcenia (tj. krzywe p-y) zasymulowano za pomocą wieloliniowych sprężyn elastycznych. Cały system, w tym konstrukcja, system kontroli wibracji i nieliniowe efekty podłoża, jest symulowany w ramach jednego trójwymiarowego modelu elementów skończonych. Dokładność modelowania została zweryfikowana przy użyciu dostępnych wyników dla turbiny wiatrowej o mocy 65 kW, omówionych w literaturze. Wyniki analizy statycznej (pushover) wykazały, że przy założeniu o nieruchomej podstawie dochodzi do przeszacowania sztywności w porównaniu z przypadkiem, w którym uwzględniono efekty SSI. Ponadto zaobserwowano, że wydajność tłumika TMD jest silnie zależna od jego dostrojonej domeny częstotliwości, a jego efektywność znacznie spada po uwzględnieniu efektów SSI. Odkształcenia poziome turbiny wiatrowej są znacznie większe w porównaniu z warunkami nieruchomej podstawy. Dlatego efekty SSI odgrywają kluczową rolę w projektowaniu turbin wiatrowych i nie powinny być pomijane w praktyce.

Słowa kluczowe: analiza dynamiczna, krzywe p-y, analiza statyczna (pushover), interakcja konstrukcji z podłożem, dynamiczny tłumik drgań, turbina wiatrowa

1. INTRODUCTION

Often, in practice structural and geotechnical designs are covered by two different teams who do not communicate effectively together. Nevertheless, realistic modeling of special structures like wind turbines which undergo various uncertain loading

*Tampere University, Finland, e-mail: a.vatanshenas@gmail.com

conditions requires a unified design strategy. This paper aims to provide an overall understanding of soil-structure interaction effects on the response of wind turbines via investigating a case study. The paper is organized as follows: First, a brief overview of previous studies is presented to clarify the theoretical background and challenges existing in the field. Next, a three dimensional numerical model is analyzed based on test results related to an actual wind turbine tested using a shake table device at the University of California, San Diego (UCSD). Validation is done by comparison of accelerations applied to different parts of the wind turbine under Landers earthquake (1992) excitation and estimation results by the current study. Then, wind turbine capacity before and after considering soil-structure interaction effects is investigated. Soil response is modelled using nonlinear elastic force versus displacement (*p-y*) curves of a stiff clay reported in the literature. Thereafter, a control vibration system tuned based on the fundamental mode of fixed-base model is added to the structure with and without considering soil-structure interaction, and their results are compared using nonlinear time history analysis. Later, the influence of wind and wave static loads on the wind turbine is investigated. It is shown that neglecting soil-structure interaction results in a significant underestimation of displacements.

2. THEORETICAL BACKGROUND

During the past few decades, the demand for using wind turbines have been increased significantly. These structures are known for their appropriate reliability and simplicity [15]. Wind turbines like cantilever structures have a low amount of redundancy and insufficient force distribution mechanism [20]. Also, due to financial obstacles and physical limitations, research on wind turbines has been mostly narrowed to numerical investigations [20]. However, few test results for these unique structures are available [29, 31-34, 37]. As shown in Equation 1, power produced by wind P, is dependent on air density ρ, rotor swept area A, and wind velocity V, where the latter is the dominant parameter. Therefore, as a rule of thumb, higher and bigger wind turbines are preferred.

$$P = \frac{1}{2}\rho A V^3 \qquad (1)$$

Around 90% of offshore wind turbines are installed in Europe [40]. What makes offshore wind turbines unique is the high amount of uncertainties related to their loading conditions. Consequently, wind turbines design demands, considering too many load combinations. Hence, reducing computational time and effort is essential [12]. In general, wind turbines are affected by quasi-static (i.e., self-weight), wind, transient (i.e., start, stop, and emergency break down), rotor cyclic [12] and, intense ground motion loads. Usually, three design strategies are utilized in designing offshore wind turbines: Soft-soft (i.e., the resonance frequency of the structure is less than harmonic frequency equal to the rotor (1P) and the wave frequencies), Soft-stiff (i.e., the resonance frequency is in the range between the 1P and the blade passing frequency 3P), and Stiff-stiff (i.e., the resonance frequency is higher than the 3P) [12]. Note that 1P and 3P are around 0.12–0.3 Hz and 0.35–0.9 Hz, respectively. However, usually, soft-stiff approach is chosen for design since the stiff-stiff design is not economical, and wave loading might cause wave fatigue for the soft-soft case [12]. Load frequencies for some wind turbines are shown in Figure 1. As shown in this figure, wind turbines undergo a vast domain of loading conditions, which makes the design procedure difficult.

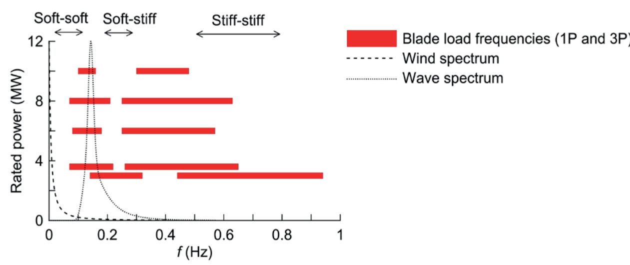

Fig. 1. Various loading frequencies for wind turbines after [2, 4], modified from [39]

In practice, the effect of earthquake loading is usually underestimated in the design process. The main reason for this issue can be the observation of limited damaged turbines under strong ground motions like North Palm Springs and Tōhoku events [1, 6, 42]. One research considering 300 earthquake records with a variety of properties (i.e., duration, frequency content, magnitude, distance from the epicenter, etc.) studied period range of wind turbines in response acceleration versus period results [19]. As illustrated in Figure 2, their findings revealed that wind turbines show similar trends as self-isolated structures due to their high natural periods, and they go under negligible lateral earthquake forces. Some studies pointed out that simple models are capable of modeling these cantilever-shape structures adequately compared to complex models [7, 27]. However, other studies like [16] indicated that strong ground motion effects are not negligible. The main reason for such a point of view is the importance of serviceability performance (i.e., controlling large displacements). For instance, a study showed a 40% surpass of lateral displacement limit based on Chinese regulation for tall structures [14, 41].

Moreover, some studies pointed out the vulnerability potential of wind turbines under vertical earthquake loading due to their low natural period in this direction [21, 35]. Consequently, the acceleration applied at the base of the tower is amplified considerably and threatens important parts like Nacelle. For instance, a study mentioned three and almost eight times the amplification of base tower acceleration for soft and rocky foundations, respectively [23]. Therefore, investigating base condition effects on the response of wind turbines is of utmost importance. SSI effects on wind turbine structure are studied in this paper.

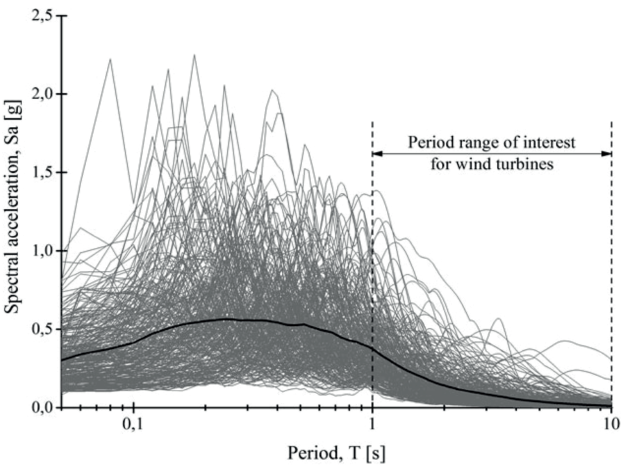

Fig. 2. Wind turbines domain in response to acceleration versus period plots, obtained from [19]

3. MODEL VERIFICATION

In this section, modeling of a wind turbine produced in Denmark, which has been tested using a shake table device at the University of California, San Diego (UCSD) under Landers earthquake (1992), is validated. This turbine is small compared to already existing wind turbines but represents fundamental aspects of these unique structures. The turbine is parked in such a way that one of the blades is toward the downside parallel to the tower direction. Wind turbine schematic and its structural properties are shown in Figure 3 and Table 1. More information regarding the test procedure is referred to [31-34].

The model is made using fully integrasted frame elements with fully fixed support at the base and the maximum mesh size of around 1 m. The tower steel has the modulus elasticity of 200 GPa, Poission's ratio of 0.3, and yield strength of 0.27 GPa. The bolades and nacelle are also modelled with materials with modulus elasticities of 0.0981 GPa and 210 GP*a*, respectively. More inforamtion about the material properties is referred to [23].

a)

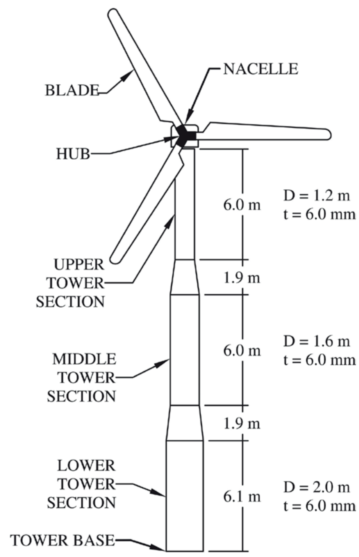

b)

Fig. 3. Wind turbine dimensions (a) and its in situ schematic (b), (source [32, 34])

Table 1. Considered wind turbine characteristics, modified from [31]

Property	Value
Rated power	65 kW
Rated wind speed	33.8 km/h
Rotor diameter	16.0 m
Tower height	21.9 m
Lower section length	7.9 m
Lower section diameter	2.0 m
Middle section length	7.9 m
Middle section diameter	1.6 m
Top section length	6.0 m
Top section diameter	1.1 m
Tower wall thickness	Around 6 mm
Rotor hub height	22.6 m
Tower mass	6400 kg
Nacelle mass	2400 kg
Rotor mass (with hub)	1900 kg
Damping	1%

Moreover, natural frequencies and mode shapes of the tested structure using OpenSees in the literature [32] and results achieved in this study presented in Figure 4 are quite similar. Moreover, a comparison between the estimated acceleration time series of different points on the wind turbine obtained in this study and video photogrammetry techniques, as well as numerical simulations in previous studies, indicates acceptable modeling accuracy (Fig. 5). Notice that acceleration induced at the base of the tower was amplified significantly in Nacelle, which can interrupt turbines' adequate performance. Hence, implementing control vibration systems to mitigate structural responses to the wind turbine is needed.

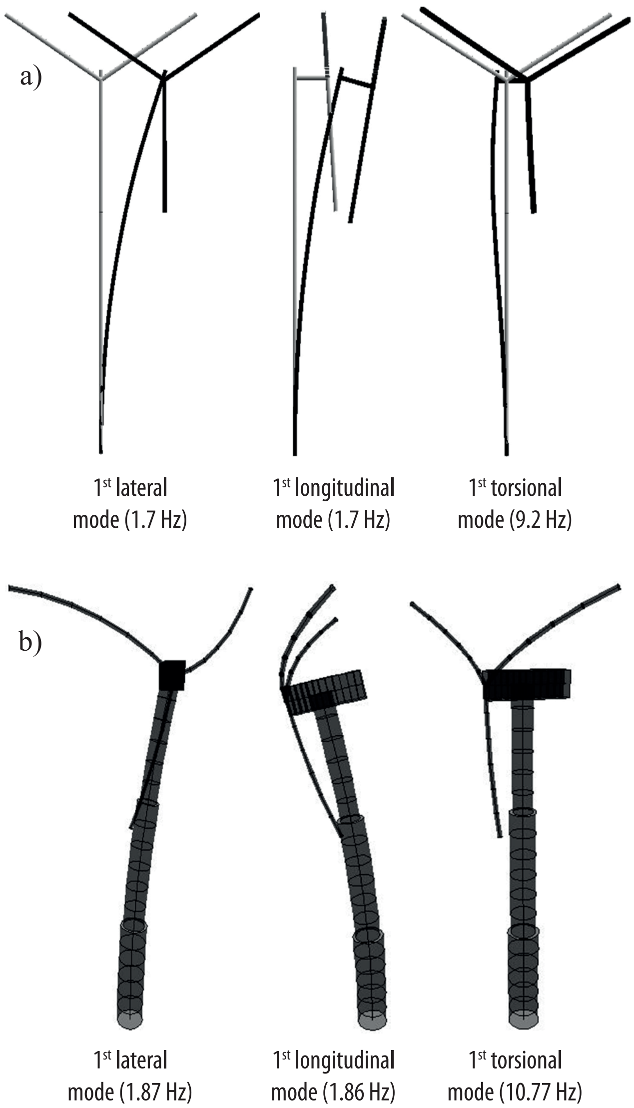

Fig. 4. Comparison between natural frequencies of considered wind turbine obtained using OpenSees (a) [32] and, obtained results in this study (b)

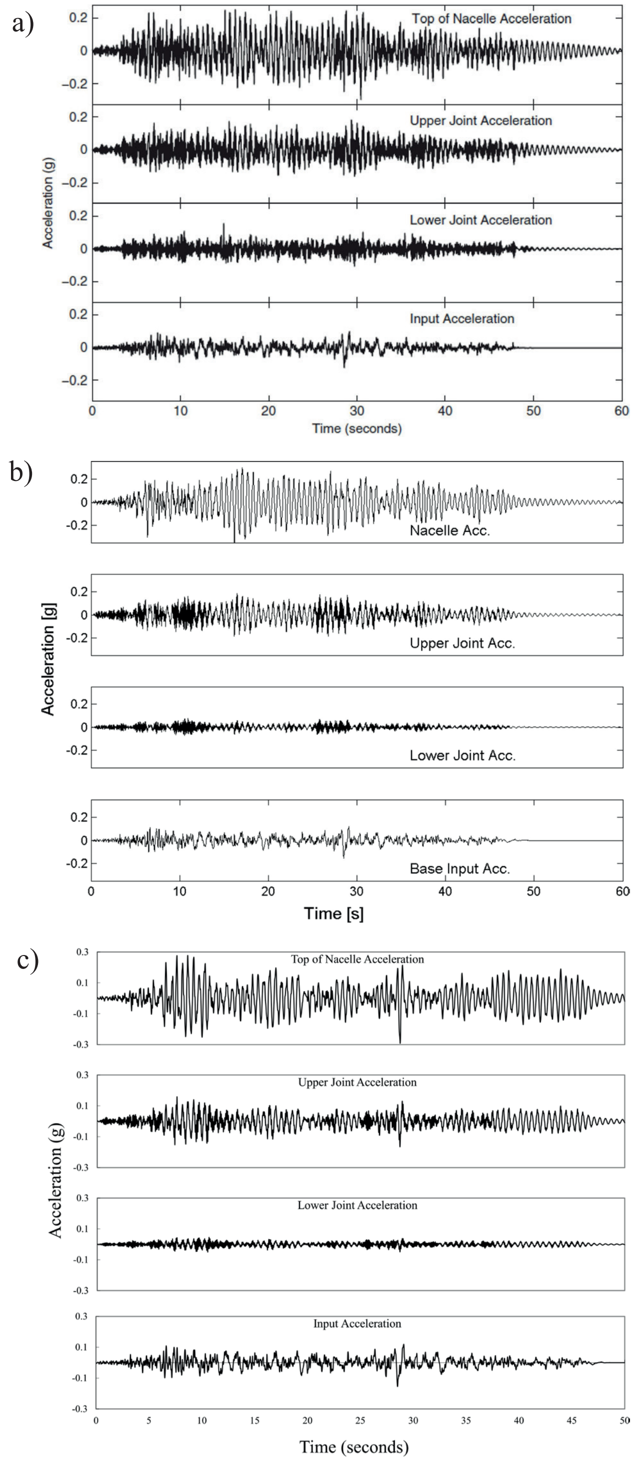

Fig. 5. Comparison of acceleration time history between experimental results (a) [32], numerical model from literature (b) [23] and, this study (c)

4. SOIL-STRUCTURE INTERACTION (SSI) EFFECTS

So far, it was assumed that the base structure is fixed to the ground. In most cases, by taking SSI effects into account, the frequency of the structure decreases, and simultaneously damping increases [17]. As a result, it is usually considered as a beneficial aspect in designing structures [38]. However, this is a crucial assumption specifically for wind turbines which undergo a wide range of dynamic loading frequencies. By neglecting SSI effects, principal frequencies and damping might be different than what was calculated for fixed-base structure [26]. For instance, Figure 6 illustrates the difference in structural performance under two cases of with and without considering SSI effects. It is apparent that simplicity in modeling might overlook additional displacements in practice [17]. Nevertheless, SSI effects are usually neglected in many cases due to complexities (i.e., nonlinear soil behavior, the right strategy for modeling, choosing appropriate software, etc.) and case dependency aspects [38].

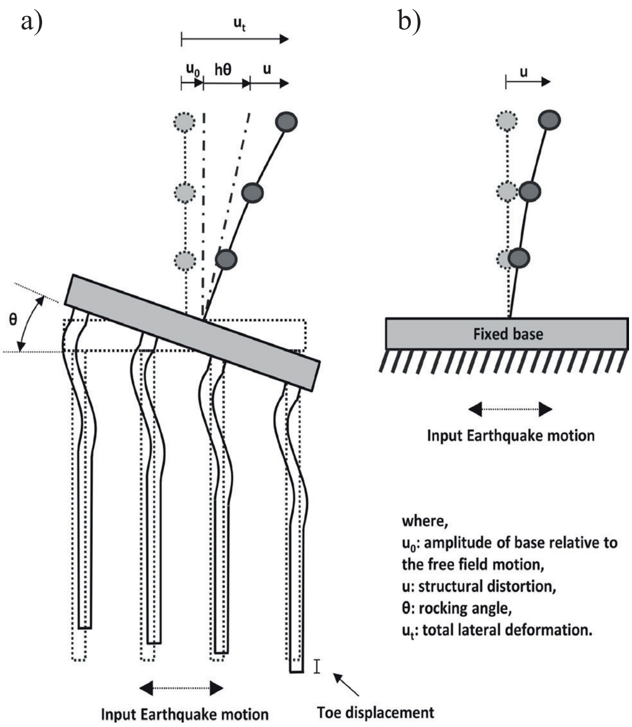

Fig. 6. Structural behavior under two cases of deformable (a) and fixed-base (b), modified from [17]

Soil behavior was shown to be highly nonlinear in terms of stiffness and damping [24]. This nonlinear behavior is affected by many parameters like plasticity index, confining stress, void ratio, etc. However, soil nonlinearity itself, considering very small, small, and large strains are out of the scope in this study and is referred to [8, 13, 43]. One of the most common methods to model SSI effects considering soil nonlinearity is force-displacement (i.e., *p-y* curves) concept introduced in the late 50s by [28]. In this method, nonlinear soil behavior is defined via multilinear elastic or plastic springs (depending on the type of analysis and model complexities). This approach is relatively simple, with the advantage of fast computing procedure. However, the drawback of this method is the lack of continuous modeling of soil layers [22]. In this research, a general approach is utilized for considering soil-pile interaction by modeling and analyzing the whole system (i.e., wind turbine, foundation, pile, soil springs, proper boundary condition, etc.) within a constant platform. Lateral force-displacement data (i.e., *p-y* curves) used in this study are gathered from previous study in the literature [3]. Soil type is a stiff clay, and bedrock is located 10 m beneath the ground surface. As shown in Figure 7, force values increase with depth until reaching a certain level, and softening occurs between 0.005 until 0.015 m.

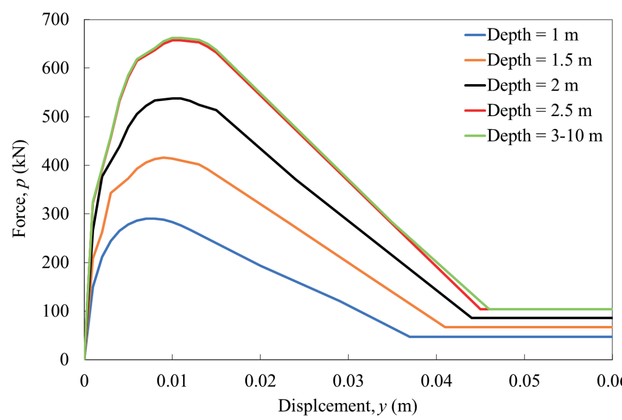

Fig. 7. Force versus displacement (i.e., p-y) graphs, (source [3])

Moreover, displacement control pushover analysis is utilized to evaluate the wind turbine's performance rather more sophisticated time history analysis, which needs unloading data as well. Pushover analysis exposes predefined lateral load to the wind turbine and increases the load step by step until reaching the desired displacement value [26]. It is observed that the first frequency of the structure is obtained 0.49 Hz, which is significantly different than the fixed-base structure. Moreover, as shown in Figure 8, the capacity curve obtained from pushover analysis under the case in which SSI effects are taken into account gives a softer response compared to the fixed-base structure. Note that more ductile behavior does not necessarily mean beneficial in terms of wind turbines with highly uncertain loading conditions. Therefore, modeling these slender structures with considering SSI effects is highly recommended.

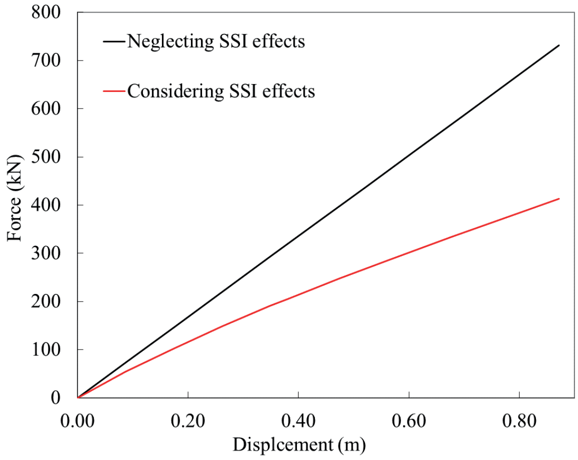

Fig. 8. Capacity curves for two cases of with and without taking SSI effects into account

5. CONTROL VIBRATION SYSTEM

Vibrations higher than 0.1 g can disrupt the performance of structures [18]. One of the most well-known techniques for controlling vibrations is utilizing the tuned mass damper (TMD) system. In this passive system, vibrations are controlled via additional mass oscillating in the opposite direction of base structure movements. This method is simple, economical, and independent of an external actuator and, as a result, less delay in operation compared to active systems [18]. However, more complex systems presented in literature like semi-active systems tried to increase the efficiency of this type of system and reduce delaying time [30].

The controlling force in these dampers is dependent on input acceleration to their system (i.e., TMDs are acceleration dependent), and their equation of motion is presented in Equation 2. As shown in Figure 9, the schematic of a TMD system is presented. Mass of the TMD is defined by mass ratio μ (usually a value between 0.02-0.1) given by Equation 3. Optimal frequency ratio α_{opt} and optimal damping ratio ξ_{opt} used in this study are obtained by Equations 4-5 available in the literature [10]. However, there are other empirical relations and techniques proposed by other researchers to tune TMD parameters, mostly their differences originate from uncertainty in considering loading conditions or accuracy of modeling [5, 25]. TMD is modlled using a link (i.e., spring) element in the model. Loading induced to the structure is five cycles of sine-shape dynamic load with the frequency corresponding to the first mode of the structure (1.87 Hz), and μ is set to 0.05. As illustrated in Figures 10 and 11, under the fixed-base assumption, a wind turbine with TMD decreased the displacements (around six times) of the Nacelle over the whole loading time. Moreover, input energy also decreased remarkably after adding TMD to the base structure (around 19 times). Nevertheless, by considering SSI effects, the same TMD did not show adequate performance and even increased the structural response in the early stages of loading. TMD performance is not much satisfactorily out of its tuned frequency. Therefore, other methods like adaptable control vibration systems or using multiple TMDs are proposed in the literature to cover this disadvantage [9].

$$m\ddot{x} + c\dot{x} + kx = -m\ddot{u} \tag{2}$$

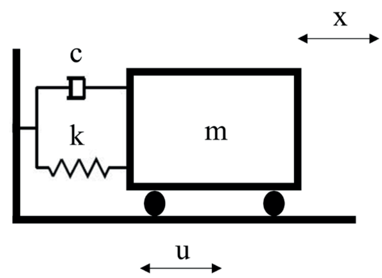

Fig. 9. Tuned mass damper (TMD) modeled as a simple single degree of freedom system

$$\mu = \frac{TMD\ mass}{Total\ mass} \tag{3}$$

$$\alpha_{opt} = \frac{1}{1+\mu} \tag{4}$$

$$\xi_{opt} = \sqrt{\frac{3\mu}{8(1+\mu)^3}} \tag{5}$$

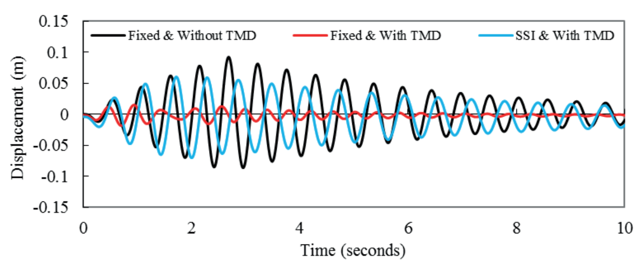

Fig. 10. Comparison of nacelle displacement concerning base condition and control vibration system

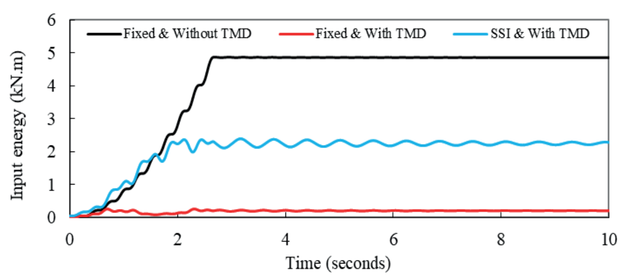

Fig. 11. Comparison of input energy concerning base condition and control vibration system

6. WAVE AND WIND LOADS

Unfortunately, due to lack of data related to taller wind turbines, only the effects of wave and wind loads of a hypothetical condition on the low-rise 65 kW wind turbine are investigated in the following. It should be noted that in practice, much taller structures are used for offshore cases, but methodologies discussed here are the same as for the taller wind turbines. As mentioned earlier, wind turbines loading conditions are sophisticated, with a high degree of uncertainty and variability. However, details of loading conditions itself are not studied in this research, and both wave and wind loads are calculated using the API recommended practice [11]. The wave force is obtained by Equations 6 and 7, known as Morison's approach. In these equations F_H is hydrodynamic force per unit length, F_D is drag force per unit length, F_I is inertia force per unit length, C_D is drag coefficient, W is weight density of water, g is gravity acceleration, A is projected area normal to element axis per unit length, V is displaced volume per unit length, U is component of the water particle velocity applying normal to the axis of the element, C_M is the inertia coefficient, dU/dt is the water particle acceleration. The wave loads are distributed along with the structural elements between mudline and wave surface.

$$F_H = F_D + F_I \tag{6}$$

$$F_H = C_D \frac{W}{2g} AU\left|U\right| + C_M \frac{W}{g} V \frac{dU}{dt} \tag{7}$$

The design wind load is also given by Equation 8 in which $U(z)$ is the one-hour mean wind velocity (*ft/s*) at height z. I_u is turbulence intensity at height z. $U(z)$ and I_u are computed by Equations 9 and 10, respectively.

$$u(z,t) = U(z)\left[1 - 0.41 I_u(z)\ln\left(\frac{t}{t_0}\right)\right] \tag{8}$$

$$U(z) = U_0\left[1 + \left(0.0573\sqrt{1 + 0.0457U_0}\right)\ln\left(\frac{z}{32.8}\right)\right] \tag{9}$$

$$I_u(z) = 0.06\left[1 + 0.0131U_0\right]\left(\frac{z}{32.8}\right)^{-0.22} \tag{10}$$

Moreover, wind drag force is calculated utilizing Equation 11 where F_W is wind force, ρ is the density of air (*slugs/ft*^{3}), u is wind speed (*ft/s*), C_S is shape coefficient, and A is an area of the object (*ft*^{2}).

$$F_W = \left(\frac{\rho}{2}\right)u^2 C_S A \tag{11}$$

All in all, the assumptions and characteristics used for wave and wind loads used in this research are presented in Table 2. Also, wave pressure and its horizontal wave velocity are illustrated in Figure 12.

Table 2. Wave and wind load characteristics investigated in this study

Property	Value
One-hour mean wind speed at 32.8 ft	30 m/s
Wind average period	600 s
Wave theory	Airy (linear)
Wave height	1.5 m
Wave period	12 s
Stormwater depth	7.5 m
Wave kinematic factor	1
Number of wave crest positions considered	1
Global height coordinate of vertical datum	7.5 m
Mudline from datum	-7.5 m

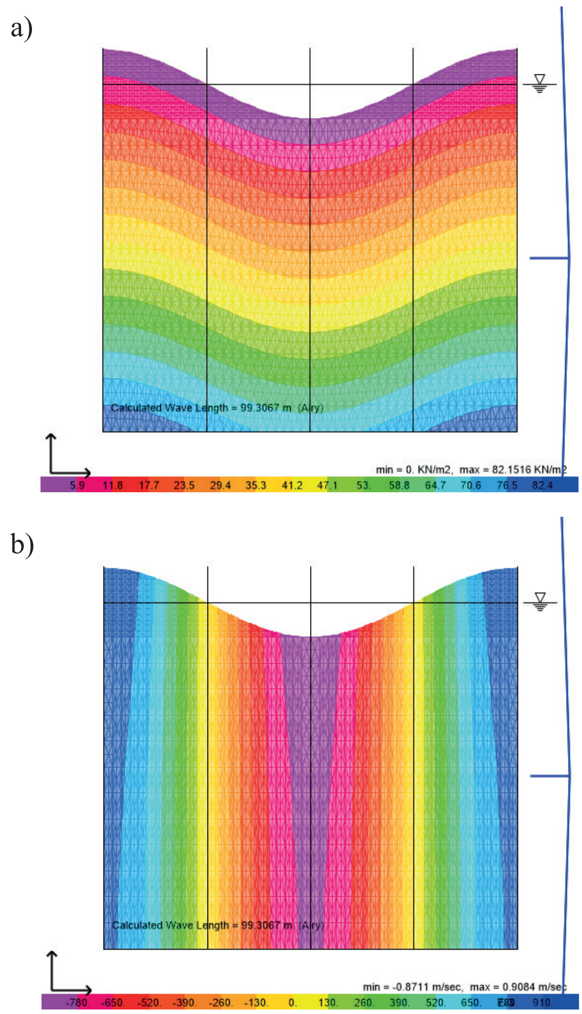

Fig. 12. Schematic of defined wave load: pressure (a), horizontal wave velocity (b)

As shown in this figure, maximum pressure and horizontal velocity occur near the mudline and at the side of the wave load, respectively. Moreover, as expected, the lateral displacement of the wind turbine in the case where SSI is taken into account is much more compared to the simplified fixed-base condition (Fig. 13). The main reason for such a significant difference in displacement values between two considered cases is that where SSI effects are considered, deformations are affected by both relative and absolute movements. Still, in fixed-base condition, absolute movements of the wind turbine are neglected.

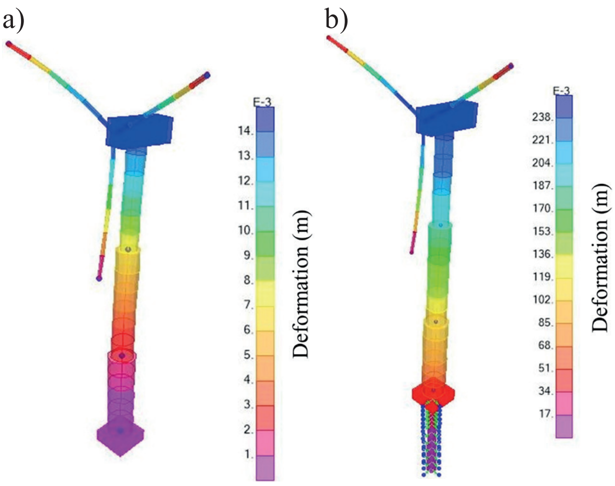

Fig. 13. Wind turbine deformation under a wave and wind load in two cases of a fixed-base (a) and considering SSI effects (b)

7. CONCLUSIONS

A 65 kW wind turbine was discussed in this study. A three-dimensional finite element model of the real wind turbine was validated based on a comparison between principal frequencies and acceleration applied to different parts of the structure. SSI effects were taken into account by modeling *p-y* curves utilizing multilinear springs. Capacity curves showed a fixed-base model acts stiffer than other model in which SSI effects were considered. Also, TMD was added to the models to decrease structural responses. However, it was shown that TMD does not perform satisfactorily out of its tuned frequency domain. Therefore, considering SSI effects is highly recommended before tuning TMD properties.

Moreover, wind turbine's behavior was investigated under wave and wind loads. It was observed that a flexible-base structure deformed more than the fixed-base structure. All in all, implementing simplified models will have significant drawbacks, such as underestimating displacements and incorrect tuning parameters for control vibration systems. Therefore, SSI effects are an essential part of wind turbines design procedure and shall not be neglected. To develop the current study, it is suggested to investigate soil-structure interaction effects on taller wind turbines. In addition, wind turbine's response utilizing adaptable control vibration system and multiple TMDs are recommended for future studies.

REFERENCES

[1] Arakawa C., Ueda Y. (2012): *Development of wind power in Japan after disaster of earthquake and Fukushima accident*. [in] Proceedings of the European Wind Energy Association Annual Event, Copenhagen, Denmark, 2012.

[2] Arany L., Bhattacharya S., Macdonald J.H., et al. (2016): *Closed form solution of Eigen frequency of monopile supported offshore wind turbines in deeper waters incorporating stiffness of substructure and SSI*. Soil Dynamics and Earthquake Engineering. 1(83): 18-32.

[3] Babakhani B., Saffar Yosefi Fard H. (2019): *Advanced structural modeling techniques with SAP2000*. Pardis-Elm Publications.

[4] Bak C., Zahle F., Bitsche R., et al. (2013): *The DTU 10-MW reference wind turbine*. In Danish Wind Power Research.

[5] Bakre S.V., Jangid R.S. (2007): *Optimum parameters of tuned mass damper for damped main system. Structural Control and Health Monitoring.* The Official Journal of the International Association for Structural Control and Monitoring and of the European Association for the Control of Structures 14(3): 448-470.

[6] Butt U.A., Ishihara T. (2012): *Seismic load evaluation of wind turbine support structures considering low structural damping and soil structure interaction.* European wind energy association annual event. April 2012, pp. 16-19.

[7] Bazeos N., Hatzigeorgiou G.D., Hondros I.D., et al. (2002): *Static, seismic and stability analyses of a prototype wind turbine steel tower.* Engineering structures 24 (8): 1015-1025.

[8] Carlton B.D., Pestana J.M. (2012): *Small strain shear modulus of high and low plasticity clays and silts*. [in.] 15th World Conference on Earthquake Engineering, Lisbon, Portugal.

[9] Clark A.J. (1988): *Multiple passive tuned mass dampers for reducing earthquake induced building motion*. [in] Proceedings of the 9th world conference on earthquake engineering, Tokyo-Kyoto, Japan 2 Aug 1988 (Vol. 779, p. 784).

[10] Connor J.J. (2003): *Structural Motion Control*, Pearson Education, Inc.

[11] CSI. SAP2000 v14 (2008) Calculation of wave load values, Technical note. California: CSI (Computers and Structures Inc.) Berkley.

[12] Damgaard M., Zania V., Andersen L.V., et al. (2014): *Effects of soil–structure interaction on real time dynamic response of offshore wind turbines on monopiles*. Engineering Structures. 15(75): 388-401.
[13] Darendeli M.B. (2001): *Development of a new family of normalized modulus reduction and material damping curves.*
[14] GB 50135:2006 (2006) Code for design of High-rise Structures. Beijing, China.
[15] Hau E. (2006): *Wind Turbines: Fundamentals. Technologies*, Application, Economics–2nd edition–Springer-Verlag Berlin Heidelberg.
[16] He G., Li J. (2008): *Seismic analysis of wind turbine system including soil-structure interaction*. [in] Proceedings of the 14th World Conference on Earthquake Engineering Jan 2008.
[17] Hokmabadi A.S., Fatahi B., Samali B. (2014): *Assessment of soil–pile–structure interaction influencing seismic response of mid-rise buildings sitting on floating pile foundations.* Computers and Geotechnics. 55: 172-186.
[18] Kareem A., Kijewski T., Tamura Y. (1999): *Mitigation of motions of tall buildings with specific examples of recent applications*. Wind and structures 2(3): 201-251.
[19] Katsanos E.I., Sextos A.G., Elnashai A.S. (2014): *Prediction of inelastic response periods of buildings based on intensity measures and analytical model parameters*. Engineering structures. 15(71): 161-177.
[20] Katsanos E.I., Thöns S., Georgakis C.T. (2016): *Wind turbines and seismic hazard: a state-of-the-art review*. Wind Energy 19(11): 2113-2133.
[21] Kaynia A.M. (2019): *Seismic considerations in design of offshore wind turbines*. Soil Dynamics and Earthquake Engineering. 1(124): 399-407.
[22] Khodair Y., Abdel-Mohti A. (2014): *Numerical analysis of pile–soil interaction under axial and lateral loads.* International Journal of Concrete Structures and Materials 8(3): 239-249.
[23] Kjørlaug R.A., Kaynia A.M., Elgamal A. (2014): *Seismic response of wind turbines due to earthquake and wind loading*. [in] Proceedings of the EURODYN 9th International Conference on Structural Dynamics, Porto, Portugal.
[24] Kondner R.L. (1963): *Hyperbolic stress-strain response: cohesive soils*. Journal of the Soil Mechanics and Foundations Division. 89(1): 115-143.
[25] Lin C.C., Ueng J.M., Huang T.C. (2000): *Seismic response reduction of irregular buildings using passive tuned mass dampers*. Engineering Structures 22(5): 513-524.
[26] Liu L., Gou W., Xie Q., et al. (2012): *Analysis of Elasto-plastic Soil-Structure Interaction System Using Pushover Method*. [in] 15th World Conference on Earthquake Engineering.
[27] Malcolm D.J., Laird D.L. (2003): *Modeling of blades as equivalent beams for aeroelastic analysis*. [in] ASME 2003 Wind Energy Symposium 1 Jan 2003 pp. 293-303. American Society of Mechanical Engineers Digital Collection.
[28] McClelland B., Focht J.A. (1956): *Soil modulus for laterally loaded piles*. Journal of the Soil Mechanics and Foundations division. [in] Proceedings of the American society of civil engineers Vol. 1, p. 22.
[29] Molinari M., Pozzi M., Zonta D., et al. (2011): *In-field testing of a steel wind turbine tower*. [in] Structural Dynamics and Renewable Energy Volume 1 (pp. 103-112). Springer, New York, NY.
[30] Nagarajaiah S., Varadarajan N. (2005): *Short time Fourier transform algorithm for wind response control of buildings with variable stiffness TMD.* Engineering Structures 27(3): 431-441.
[31] Prowell I., Veletzos M., Elgamal A., et al. (2008): *Shake table test of a 65 kW wind turbine and computational simulation*. [in] 14th World Conference on Earthquake Engineering, Beijing, China 12 Oct (pp. 12-17).
[32] Prowell I., Veletzos M., Elgamal A., et al. (2009): *Experimental and numerical seismic response of a 65 kW wind turbine.* Journal of Earthquake Engineering 13(8): 1172-1190.
[33] Prowell I., Uang C.M., Elgamal A., et al. (2012): *Shake table testing of a utility-scale wind turbine.* Journal of engineering mechanics. 138(7): 900-909.
[34] Prowell I., Elgamal A., Uang C.M., et al. (2014): *Shake table testing and numerical simulation of an utility-scale wind turbine including operational effects*. Wind Energy. 17(7): 997-1016.
[35] Ritschel U., Warnke I., Kirchner J., et al. (2003): *Wind turbines and earthquakes*. [in] 2nd World Wind Energy Conference, Cape Town, South Africa Nov 2003, pp. 1-8. Cape Town: World Wind Energy Association.
[36] RP2A-WSD AP (2000): Recommended practice for planning, designing and constructing fixed offshore platforms–working stress design. American Petroleum Institute, Washington Dc.
[37] Schreck S.J., Robinson M.C., Hand M.M., et al. (2001): *Blade dynamic stall vortex kinematics for a horizontal axis wind turbine in yawed conditions*. J. Sol. Energy Eng. 123(4): 272-281.
[38] Sextos A.G., Pitilakis K.D., Kappos A.J. (2003): *Inelastic dynamic analysis of RC bridges accounting for spatial variability of ground motion, site effects and soil–structure interaction phenomena. Part 1: Methodology and analytical tools*. Earthquake engineering & structural dynamics. 32(4): 607-627.
[39] Skau K.S., Page A.M., Kaynia A.M., et al. (2018): *REDWIN–REDucing cost in offshore WINd by integrated structural and geotechnical design.* [in] IOP Conference Series-Journal of Physics, EERA DeepWind.

environment

[40] Smith A., Stehly T., Musial W. (2015): *2014-2015 offshore wind technologies market report*. National Renewable Energy Lab.(NREL), Golden, CO United States, Sep 1.

[41] Song B., Yi Y., Wu J.C. (2013): *Study on seismic dynamic response of offshore wind turbine tower with monopile foundation based on M method.* In Advanced Materials Research Vol. 663, pp. 686-691. Trans Tech Publications Ltd.

[42] Swan S., Hadjian A.H. (1988): *The 1986 North Palm Springs earthquake: effects on power facilities* (No. EPRI-NP-5607) EQE, Inc., San Francisco, CA (USA) Bechtel Power Corp, Norwalk, CA (USA).

[43] Vatanshenas A. (2024): *Nonlinear Soil-structure Interaction of Bridges: Practical Approach Considering Small Strain Behaviour.* Doctoral Thesis, Tampere University. ISBN: 978-952-03-3234-1.